Gravitational Waves from the Early Universe

Lecture 1B: Gravitational Waves, Experiments

Kai Schmitz (CERN)

Chung-Ang University, Seoul, South Korea | June 2 – 4

Global network of GW detectors

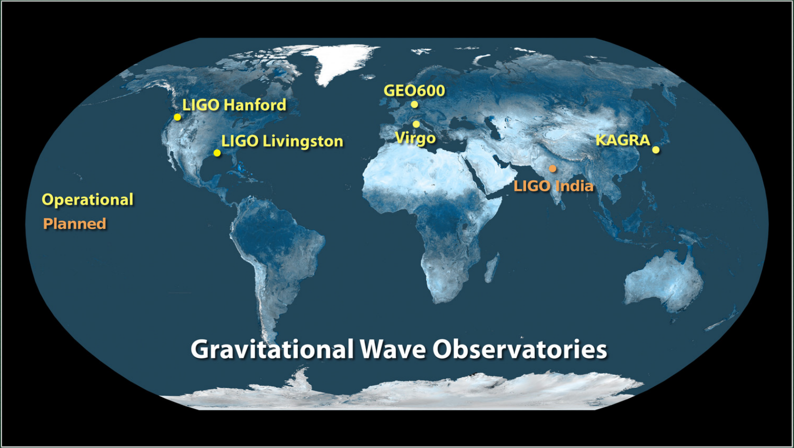

[ligo.caltech.edu]

Ground-based GW laser interferometers:
Generation 1: GEO600, LIGO, TAMA, Virgo
Generation 2: Advanced LIGO (Laser Interferometer Gravitational-Wave Observatory) / Virgo
Generation 2.5: KAGRA (Kamioka Gravitational Wave Detector), underground and cryogenic

On the eve of multifrequency GW astronomy

Ground	Space	Sky

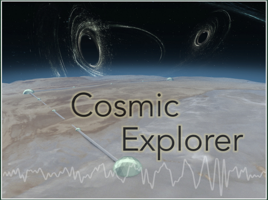

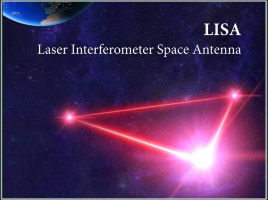

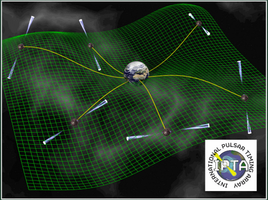

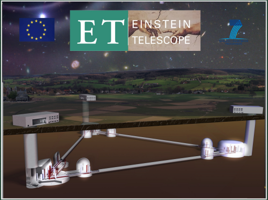

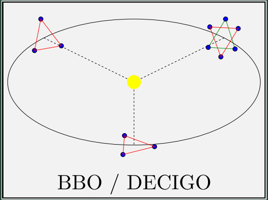

$f \sim 10 \cdots 1000\,\mathrm{Hz}$ | $f \sim 1 \cdots 1000\,\mathrm{mHz}$ | $f \sim 1 \cdots 10\,\mathrm{nHz}$

Plus: AEDGE, AION, MAGIS, TaiJi, TianQin, ...
Plus: Future measurements of CMB polarization and spectral distortions

Outline Lecture 1B

1. GW interferometers
2. Experimental sensitivity
3. Pulsar timing arrays
4. Cosmic microwave background
5. Summary

Transient GW signals

GW passing a Michelson interferometer

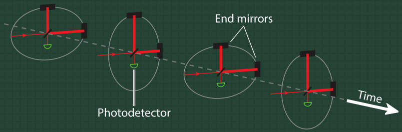

[Ballmer, Mandic: Ann. Rev. Nucl. Part. Sci. **65** (2015) 555]

Chirp signal in the LIGO / Virgo detectors

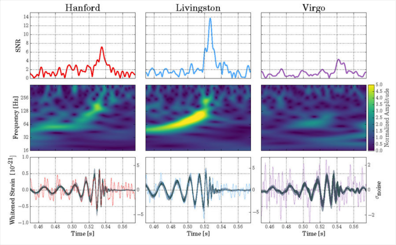

[ligo.caltech.edu]

Transient GW signals

GW passing a Michelson interferometer

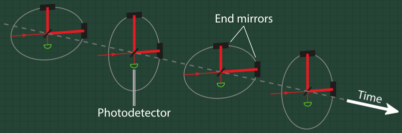

[Ballmer, Mandic: Ann. Rev. Nucl. Part. Sci. **65** (2015) 555]

Chirp signal in the LIGO / Virgo detectors

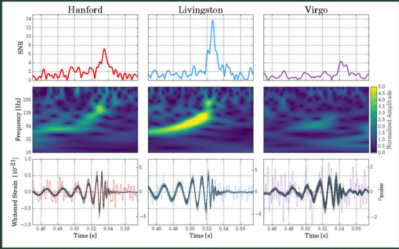

[ligo.caltech.edu]

Signal seen by the detector: Convolute h_{ij} with impulse response R^{ij} (detector geometry)

$$s(t) = \int_{-\infty}^{\infty} dt' \int d^3\boldsymbol{x}' R^{ij}(t', \boldsymbol{x}')\, h_{ij}(t - t', \boldsymbol{x} - \boldsymbol{x}') \quad (1)$$

Transient GW signals

GW passing a Michelson interferometer

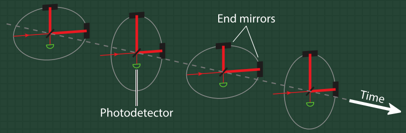

[Ballmer, Mandic: Ann. Rev. Nucl. Part. Sci. **65** (2015) 555]

Chirp signal in the LIGO / Virgo detectors

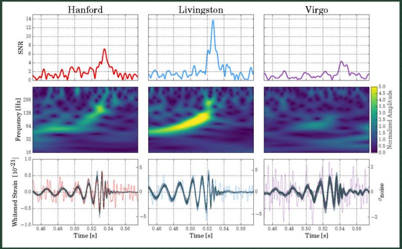

[ligo.caltech.edu]

Signal seen by the detector: Convolute h_{ij} with impulse response R^{ij} (detector geometry)

$$s(t) = \int_{-\infty}^{\infty} dt' \int d^3\boldsymbol{x}'\, R^{ij}(t', \boldsymbol{x}')\, h_{ij}(t - t', \boldsymbol{x} - \boldsymbol{x}') \tag{1}$$

Decompose incoming GW into plane-wave contributions with definite f, p, and $\boldsymbol{n}$:

$$h_{ij}(t, \boldsymbol{x}) = \sum_{p=+,\times} \int_{-\infty}^{\infty} df \int d^2\boldsymbol{n}\, h_p(f, \boldsymbol{n})\, e^p_{ij}(\boldsymbol{n})\, e^{2\pi i f(t - \boldsymbol{n}\boldsymbol{x})} \tag{2}$$

Detector response to the signal

Signal seen by the detector in the frequency domain:

$$\tilde{s}(f) = \frac{1}{2\pi} \int_{-\infty}^{\infty} dt\, s(t)\, e^{-2\pi i f t} = \sum_{p=+,\times} \int d^2\boldsymbol{n}\, R_p(f, \boldsymbol{n})\, h_p(f, \boldsymbol{n}) \qquad (3)$$

Detector response to the signal

Signal seen by the detector in the frequency domain:

$$\tilde{s}(f) = \frac{1}{2\pi}\int_{-\infty}^{\infty} dt\, s(t)\, e^{-2\pi i f t} = \sum_{p=+,\times} \int d^2\boldsymbol{n}\, R_p(f,\boldsymbol{n})\, h_p(f,\boldsymbol{n}) \tag{3}$$

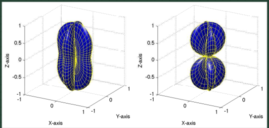

[Cornish, Romano: 1608.06889]

Antenna patterns:
Graphs of $|R_p(f,\boldsymbol{n})|$ as functions $\boldsymbol{n}$ at fixed f.

Can be computed based on changes in the light-travel time between test masses at the end of the interferometer arms.

Detector response to the signal

Signal seen by the detector in the frequency domain:

$$\tilde{s}(f) = \frac{1}{2\pi}\int_{-\infty}^{\infty} dt\, s(t)\, e^{-2\pi i f t} = \sum_{p=+,\times} \int d^2\boldsymbol{n}\, R_p(f,\boldsymbol{n})\, h_p(f,\boldsymbol{n}) \tag{3}$$

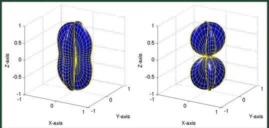

[Cornish, Romano: 1608.06889]

Antenna patterns:
Graphs of $|R_p(f,\boldsymbol{n})|$ as functions $\boldsymbol{n}$ at fixed f.

Can be computed based on changes in the light-travel time between test masses at the end of the interferometer arms.

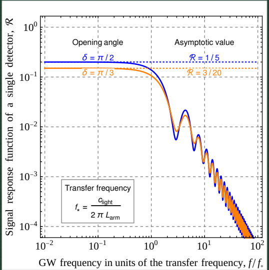

Signal response / detector transfer function:
Average over the square of the antenna patterns.

$$\mathcal{R} = \frac{1}{2}\sum_p \frac{1}{4\pi}\int d^2\boldsymbol{n}\, |R_p(f,\boldsymbol{n})|^2 \tag{4}$$

Quantifies loss in sensitivity due to the fact that, on average, GWs do not arrive from the optimal direction.

Searching for a stochastic GW background

Detector data stream composed of signal and noise contributions: $d(t) = s(t) + n(t)$

Searching for a stochastic GW background

Detector data stream composed of signal and noise contributions: $d(t) = s(t) + n(t)$

Noise characterized by detector noise power spectrum $D_{\rm noise}$:

$$\langle n^2(t)\rangle = \int_0^\infty df\, D_{\rm noise}(f)\,, \qquad \langle \tilde{n}(f)\,\tilde{n}^*(f')\rangle = \frac{1}{2}\,\delta(f-f')\,D_{\rm noise}(f) \tag{5}$$

Searching for a stochastic GW background

Detector data stream composed of signal and noise contributions: $d(t) = s(t) + n(t)$

Noise characterized by detector noise power spectrum $D_{\rm noise}$:

$$\langle n^2(t) \rangle = \int_0^\infty df \, D_{\rm noise}(f) \, , \qquad \langle \tilde{n}(f) \, \tilde{n}^*(f') \rangle = \frac{1}{2} \, \delta(f - f') \, D_{\rm noise}(f) \tag{5}$$

Signal characterized by strain power spectrum S_h and detector transfer function $\mathcal{R}$:

$$\langle s^2(t) \rangle = \int_0^\infty df \, \mathcal{R}(f) \, S_h(f) \, , \qquad \langle \tilde{s}(f) \, \tilde{s}^*(f') \rangle = \frac{1}{2} \, \delta(f - f') \, \mathcal{R}(f) \, S_h(f) \tag{6}$$

Searching for a stochastic GW background

Detector data stream composed of signal and noise contributions: $d(t) = s(t) + n(t)$

Noise characterized by detector noise power spectrum $D_{\rm noise}$:

$$\langle n^2(t)\rangle = \int_0^\infty df\, D_{\rm noise}(f)\,, \qquad \langle \tilde n(f)\, \tilde n^*(f')\rangle = \frac{1}{2}\,\delta(f-f')\, D_{\rm noise}(f) \tag{5}$$

Signal characterized by strain power spectrum S_h and detector transfer function $\mathcal{R}$:

$$\langle s^2(t)\rangle = \int_0^\infty df\, \mathcal{R}(f)\, S_h(f)\,, \qquad \langle \tilde s(f)\, \tilde s^*(f')\rangle = \frac{1}{2}\,\delta(f-f')\, \mathcal{R}(f)\, S_h(f) \tag{6}$$

Challenge: Signal looks like another form of noise. Therefore, extract SGWB signal from the noisy background based on: spectral properties, temporal modulations, null channels, etc.

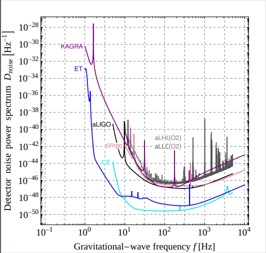

Searching for a stochastic GW background

Detector data stream composed of signal and noise contributions: $d(t) = s(t) + n(t)$

Noise characterized by detector noise power spectrum $D_{\rm noise}$:

$$\langle n^2(t)\rangle = \int_0^\infty df\, D_{\rm noise}(f)\,, \qquad \langle \tilde{n}(f)\,\tilde{n}^*(f')\rangle = \frac{1}{2}\,\delta(f-f')\,D_{\rm noise}(f) \tag{5}$$

Signal characterized by strain power spectrum S_h and detector transfer function $\mathcal{R}$:

$$\langle s^2(t)\rangle = \int_0^\infty df\, \mathcal{R}(f)\,S_h(f)\,, \qquad \langle \tilde{s}(f)\,\tilde{s}^*(f')\rangle = \frac{1}{2}\,\delta(f-f')\,\mathcal{R}(f)\,S_h(f) \tag{6}$$

Challenge: Signal looks like another form of noise. Therefore, extract SGWB signal from the noisy background based on: spectral properties, temporal modulations, null channels, etc.

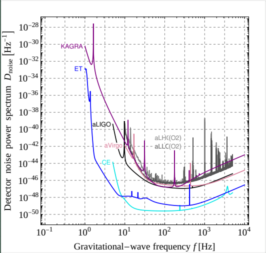

Single detector: Require $S_h \gtrsim D_{\rm noise}/\mathcal{R}$ for detection.

Searching for a stochastic GW background

Detector data stream composed of signal and noise contributions: $d(t) = s(t) + n(t)$

Noise characterized by detector noise power spectrum $D_{\rm noise}$:

$$\langle n^2(t)\rangle = \int_0^\infty df\, D_{\rm noise}(f)\,, \qquad \langle \tilde n(f)\,\tilde n^*(f')\rangle = \frac{1}{2}\,\delta(f-f')\,D_{\rm noise}(f) \tag{5}$$

Signal characterized by strain power spectrum S_h and detector transfer function $\mathcal{R}$:

$$\langle s^2(t)\rangle = \int_0^\infty df\, \mathcal{R}(f)\,S_h(f)\,, \qquad \langle \tilde s(f)\,\tilde s^*(f')\rangle = \frac{1}{2}\,\delta(f-f')\,\mathcal{R}(f)\,S_h(f) \tag{6}$$

Challenge: Signal looks like another form of noise. Therefore, extract SGWB signal from the noisy background based on: spectral properties, temporal modulations, null channels, etc.

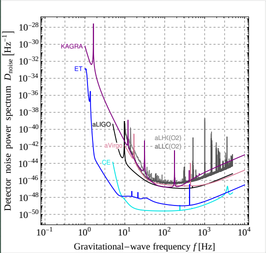

Single detector: Require $S_h \gtrsim D_{\rm noise}/\mathcal{R}$ for detection.

Detector network: Cross-correlate signal from detector pairs.

$$S_{IJ} = \int_{-T/2}^{T/2} dt \int_{-T/2}^{T/2} dt'\, d_I(t)\, Q_{IJ}(t-t')\, d_J(t') \tag{7}$$

with filter function Q_{IJ} (depends only on $t-t'$, highly localized in time). Match Q_{IJ} so as to maximize the SNR.

Optimal filtering

Expectation value of S_{IJ}, assuming uncorrelated detector noise, $\langle n_I n_J \rangle = 0$:

$$\langle S_{IJ} \rangle = \frac{T}{2} \int_{-\infty}^{\infty} df \, \widetilde{Q}_{IJ}(f) \, \Gamma_{IJ}(f) \, S_h(f) \tag{8}$$

Optimal filtering

Expectation value of S_{IJ}, assuming uncorrelated detector noise, $\langle n_I n_J \rangle = 0$:

$$\langle S_{IJ} \rangle = \frac{T}{2} \int_{-\infty}^{\infty} df\, \widetilde{Q}_{IJ}(f)\, \Gamma_{IJ}(f)\, S_h(f) \tag{8}$$

Fourier-transformed filter $\widetilde{Q}_{IJ}$ and overlap reduction function Γ_{IJ} (generalization of $\mathcal{R}$):

$$\Gamma_{IJ}(f) = \frac{1}{2} \sum_p \frac{1}{4\pi} \int d^2\boldsymbol{n}\, R_p^I(f, \boldsymbol{n})\, R_p^{J*}(f, \boldsymbol{n}) \tag{9}$$

Optimal filtering

Expectation value of S_{IJ}, assuming uncorrelated detector noise, $\langle n_I n_J \rangle = 0$:

$$\langle S_{IJ} \rangle = \frac{T}{2} \int_{-\infty}^{\infty} df\, \widetilde{Q}_{IJ}(f)\, \Gamma_{IJ}(f)\, S_h(f) \tag{8}$$

Fourier-transformed filter $\widetilde{Q}_{IJ}$ and overlap reduction function Γ_{IJ} (generalization of $\mathcal{R}$):

$$\Gamma_{IJ}(f) = \frac{1}{2} \sum_p \frac{1}{4\pi} \int d^2\boldsymbol{n}\, R_p^I(f, \boldsymbol{n})\, R_p^{J*}(f, \boldsymbol{n}) \tag{9}$$

Root mean square of the noise $N_{IJ} = S_{IJ} - \langle S_{IJ} \rangle$ (in the weak-signal approximation):

$$\langle N_{IJ}^2 \rangle^{1/2} = \left[\langle S_{IJ}^2 \rangle - \langle S_{IJ} \rangle^2 \right]^{1/2} = \left[\frac{T}{4} \int_{-\infty}^{\infty} df\, \left| \widetilde{Q}_{IJ}(f) \right|^2 D_{\mathrm{noise}}^I(f)\, D_{\mathrm{noise}}^J(f) \right]^{1/2} \tag{10}$$

Optimal filtering

Expectation value of S_{IJ}, assuming uncorrelated detector noise, $\langle n_I n_J \rangle = 0$:

$$\langle S_{IJ} \rangle = \frac{T}{2} \int_{-\infty}^{\infty} df\, \widetilde{Q}_{IJ}(f)\, \Gamma_{IJ}(f)\, S_h(f) \tag{8}$$

Fourier-transformed filter $\widetilde{Q}_{IJ}$ and overlap reduction function Γ_{IJ} (generalization of $\mathcal{R}$):

$$\Gamma_{IJ}(f) = \frac{1}{2} \sum_p \frac{1}{4\pi} \int d^2\boldsymbol{n}\, R_p^I(f, \boldsymbol{n})\, R_p^{J*}(f, \boldsymbol{n}) \tag{9}$$

Root mean square of the noise $N_{IJ} = S_{IJ} - \langle S_{IJ} \rangle$ (in the weak-signal approximation):

$$\langle N_{IJ}^2 \rangle^{1/2} = \left[\langle S_{IJ}^2 \rangle - \langle S_{IJ} \rangle^2\right]^{1/2} = \left[\frac{T}{4} \int_{-\infty}^{\infty} df \left|\widetilde{Q}_{IJ}(f)\right|^2 D_{\mathrm{noise}}^I(f)\, D_{\mathrm{noise}}^J(f)\right]^{1/2} \tag{10}$$

Optimal filter that maximizes the signal-to-noise ratio $\varrho_{IJ} = \langle S_{IJ} \rangle / \langle N_{IJ}^2 \rangle^{1/2}$:

$$\widetilde{Q}_{IJ}(f) \propto \frac{\Gamma_{IJ}(f)\, S_h(f)}{D_{\mathrm{noise}}^I(f)\, D_{\mathrm{noise}}^J(f)} \tag{11}$$

Note: $\widetilde{Q}_{IJ}$ requires knowledge of the signal one intends to measure $\rightarrow$ template banks

Overlap reduction functions

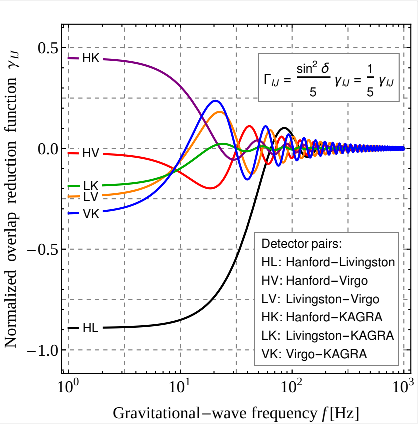

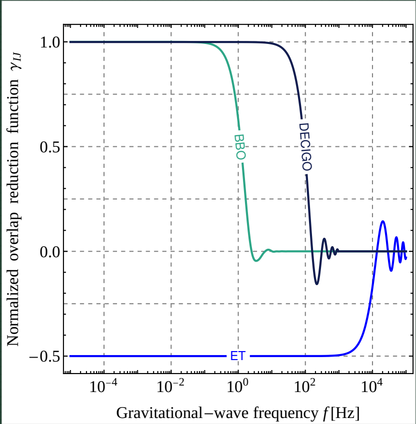

Normalization such that $\gamma_{IJ}(f=0)=1$ for a pair of identical, co-located, co-aligned detectors with opening angle δ between their two interferometer arms:

$$\gamma_{IJ}(f) = \frac{5}{\sin^2\delta}\Gamma_{IJ} \tag{12}$$

Total signal-to-noise ratio

For a network of $I, J = 1, \cdots, N_{\rm det}$ detectors:

$$\varrho = \left[\sum_{J>I} \varrho_{IJ}^2 \right]^{1/2} \quad , \qquad \varrho_{IJ} = \left[2\,T \int_{\Delta f} df \, \frac{\Gamma_{IJ}^2(f) S_h^2(f)}{D_{\rm noise}^I(f)\, D_{\rm noise}^J(f)} \right]^{1/2} \tag{13}$$

Total signal-to-noise ratio

For a network of $I, J = 1, \cdots, N_{\rm det}$ detectors:

$$\varrho = \left[\sum_{J>I} \varrho_{IJ}^2\right]^{1/2} , \qquad \varrho_{IJ} = \left[2\,T \int_{\Delta f} df\, \frac{\Gamma_{IJ}^2(f) S_h^2(f)}{D^I_{\rm noise}(f)\, D^J_{\rm noise}(f)}\right]^{1/2} \tag{13}$$

Effective strain noise power spectrum $S^{\rm eff}_{\rm noise}$ for the entire network:

$$S^{\rm eff}_{\rm noise}(f) = \left[\sum_{J>I} \frac{\Gamma_{IJ}^2(f)}{D^I_{\rm noise}(f)\, D^J_{\rm noise}(f)}\right]^{-1/2} \tag{14}$$

Total signal-to-noise ratio

For a network of $I, J = 1, \cdots, N_{\mathrm{det}}$ detectors:

$$\varrho = \left[\sum_{J>I} \varrho_{IJ}^2\right]^{1/2} \,, \qquad \varrho_{IJ} = \left[2\,T \int_{\Delta f} df \, \frac{\Gamma_{IJ}^2(f) S_h^2(f)}{D_{\mathrm{noise}}^I(f)\, D_{\mathrm{noise}}^J(f)}\right]^{1/2} \tag{13}$$

Effective strain noise power spectrum $S_{\mathrm{noise}}^{\mathrm{eff}}$ for the entire network:

$$S_{\mathrm{noise}}^{\mathrm{eff}}(f) = \left[\sum_{J>I} \frac{\Gamma_{IJ}^2(f)}{D_{\mathrm{noise}}^I(f)\, D_{\mathrm{noise}}^J(f)}\right]^{-1/2} \tag{14}$$

Express both signal and noise in terms of a GW energy density power spectrum:

$$\Omega_{\mathrm{signal}}(f) = \frac{2\pi^2}{3H_0^2}\, f^3 S_h(f) \,, \quad \Omega_{\mathrm{noise}}(f) = \frac{2\pi^2}{3H_0^2}\, f^3 S_{\mathrm{noise}}^{\mathrm{eff}}(f) \,. \tag{15}$$

Total signal-to-noise ratio

For a network of $I, J = 1, \cdots, N_{\rm det}$ detectors:

$$\varrho = \left[\sum_{J>I} \varrho_{IJ}^2\right]^{1/2} , \qquad \varrho_{IJ} = \left[2\,T \int_{\Delta f} df\, \frac{\Gamma_{IJ}^2(f) S_h^2(f)}{D_{\rm noise}^I(f)\, D_{\rm noise}^J(f)}\right]^{1/2} \tag{13}$$

Effective strain noise power spectrum $S_{\rm noise}^{\rm eff}$ for the entire network:

$$S_{\rm noise}^{\rm eff}(f) = \left[\sum_{J>I} \frac{\Gamma_{IJ}^2(f)}{D_{\rm noise}^I(f)\, D_{\rm noise}^J(f)}\right]^{-1/2} \tag{14}$$

Express both signal and noise in terms of a GW energy density power spectrum:

$$\Omega_{\rm signal}(f) = \frac{2\pi^2}{3H_0^2}\, f^3 S_h(f)\,, \quad \Omega_{\rm noise}(f) = \frac{2\pi^2}{3H_0^2}\, f^3 S_{\rm noise}^{\rm eff}(f)\,. \tag{15}$$

$$\boxed{\varrho = \left[2\,T \int_{\Delta f} df \left(\frac{\Omega_{\rm signal}(f)}{\Omega_{\rm noise}(f)}\right)^2\right]^{1/2} \propto \sqrt{N_{\rm det}(N_{\rm det}-1)\, N_{\rm bin}\, T\, \delta f}} \tag{16}$$

Integration over time and frequency boosts SNR by many orders of magnitude!

Effective strain noise power spectra

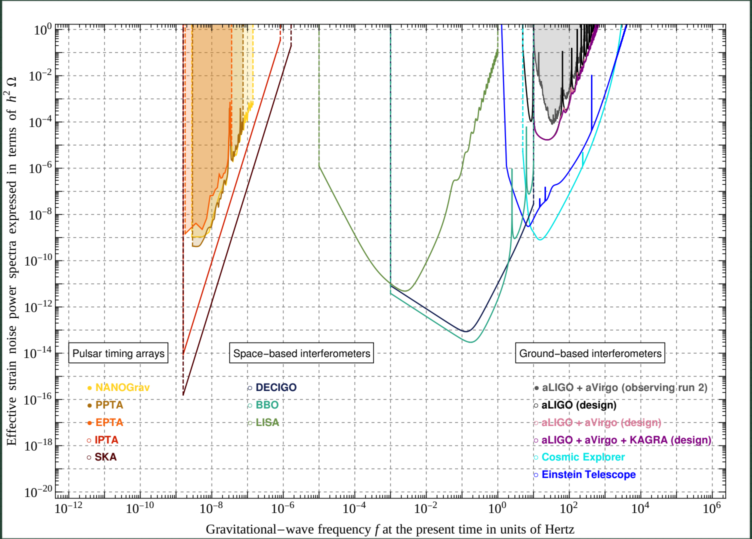

Instantaneous sensitivity, no integration over time and frequency

Sensitivity curves

Sensitivity curves[1] for the two-detector network aLIGO Hanford + aLIGO Livingston:[2]

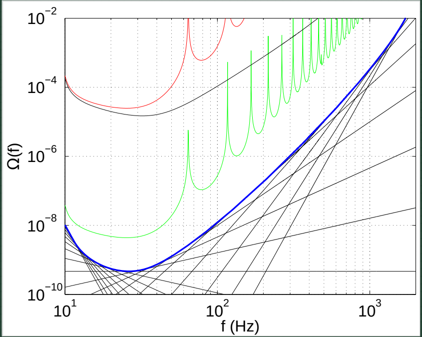

[Romano, Thrane: 1310.5300]

[1] All curves expressed in terms of Ω: the GW energy density spectrum in units of the critical energy density ρ_c.

[2] Based on slightly obsolete data for $D_{\rm noise}$: `https://dcc.ligo.org/LIGO-T0900288/public`

Sensitivity curves

Sensitivity curves[1] for the two-detector network aLIGO Hanford + aLIGO Livingston:[2]

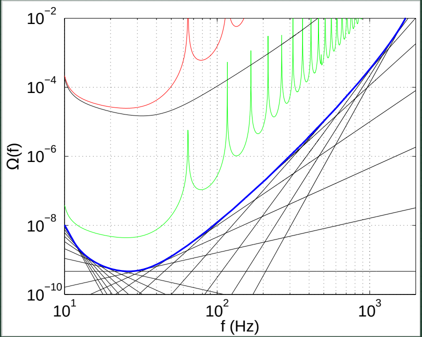

[Romano, Thrane: 1310.5300]

Black curve: Detector noise spectrum

$$D_{\rm noise}(f)$$

[1] All curves expressed in terms of Ω: the GW energy density spectrum in units of the critical energy density ρ_c.

[2] Based on slightly obsolete data for $D_{\rm noise}$: https://dcc.ligo.org/LIGO-T0900288/public

Sensitivity curves

Sensitivity curves[1] for the two-detector network aLIGO Hanford + aLIGO Livingston:[2]

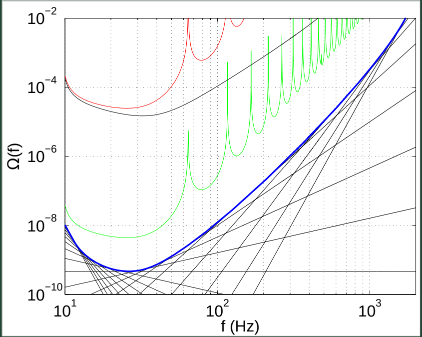

[Romano, Thrane: 1310.5300]

Black curve: Detector noise spectrum

$$D_{\rm noise}(f)$$

Red curve: Effective strain noise

$$S^{\rm eff}_{\rm noise}(f) = D_{\rm noise}(f)/\left|\Gamma(f)\right|$$

[1] All curves expressed in terms of Ω: the GW energy density spectrum in units of the critical energy density ρ_c.
[2] Based on slightly obsolete data for $D_{\rm noise}$: `https://dcc.ligo.org/LIGO-T0900288/public`

Sensitivity curves

Sensitivity curves[1] for the two-detector network aLIGO Hanford + aLIGO Livingston:[2]

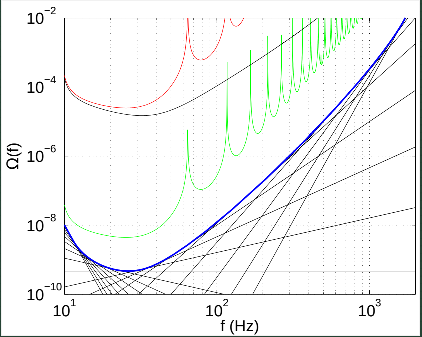

[Romano, Thrane: 1310.5300]

Black curve: Detector noise spectrum

$$D_{\rm noise}(f)$$

Red curve: Effective strain noise

$$S^{\rm eff}_{\rm noise}(f) = D_{\rm noise}(f)/\left|\Gamma(f)\right|$$

Green curve: Rescaled effective strain noise

$$S^{\rm eff}_{\rm noise}(f)/\sqrt{N_{\rm det}(N_{\rm det}-1)\,T\,\delta f}$$

[1] All curves expressed in terms of Ω: the GW energy density spectrum in units of the critical energy density ρ_c.
[2] Based on slightly obsolete data for $D_{\rm noise}$: https://dcc.ligo.org/LIGO-T0900288/public

Sensitivity curves

Sensitivity curves[1] for the two-detector network aLIGO Hanford + aLIGO Livingston:[2]

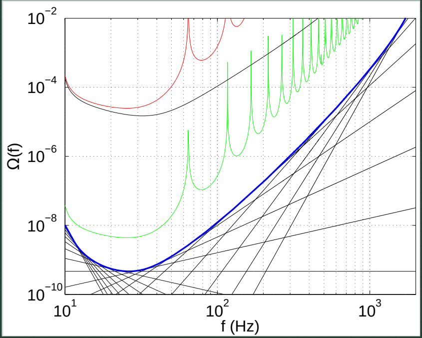

[Romano, Thrane: 1310.5300]

Black curve: Detector noise spectrum

$$D_{\rm noise}(f)$$

Red curve: Effective strain noise

$$S_{\rm noise}^{\rm eff}(f) = D_{\rm noise}(f) / \left|\Gamma(f)\right|$$

Green curve: Rescaled effective strain noise

$$S_{\rm noise}^{\rm eff}(f) / \sqrt{N_{\rm det}\left(N_{\rm det}-1\right) T\, \delta f}$$

Black straight lines: Set of power-law curves that result in $\varrho = 1$ based on Eq. (16)

[1] All curves expressed in terms of Ω: the GW energy density spectrum in units of the critical energy density ρ_c.
[2] Based on slightly obsolete data for $D_{\rm noise}$: `https://dcc.ligo.org/LIGO-T0900288/public`

Sensitivity curves

Sensitivity curves[1] for the two-detector network aLIGO Hanford + aLIGO Livingston:[2]

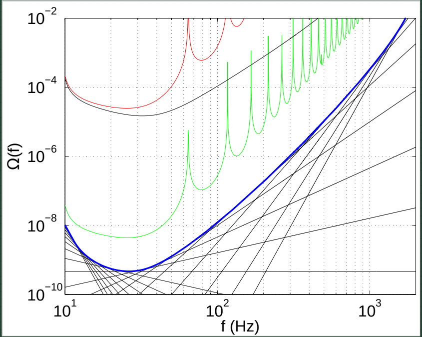

[Romano, Thrane: 1310.5300]

Black curve: Detector noise spectrum

$$D_{\rm noise}(f)$$

Red curve: Effective strain noise

$$S_{\rm noise}^{\rm eff}(f) = D_{\rm noise}(f) / \left|\Gamma(f)\right|$$

Green curve: Rescaled effective strain noise

$$S_{\rm noise}^{\rm eff}(f) / \sqrt{N_{\rm det}\left(N_{\rm det}-1\right) T\,\delta f}$$

Black straight lines: Set of power-law curves that result in $\varrho = 1$ based on Eq. (16)

Blue curve: Envelope $\rightarrow$ power-law-integrated sensitivity (PLIS) curve

---

[1] All curves expressed in terms of Ω: the GW energy density spectrum in units of the critical energy density ρ_c.

[2] Based on slightly obsolete data for $D_{\rm noise}$: `https://dcc.ligo.org/LIGO-T0900288/public`

Sensitivity curves

Sensitivity curves[1] for the two-detector network aLIGO Hanford + aLIGO Livingston:[2]

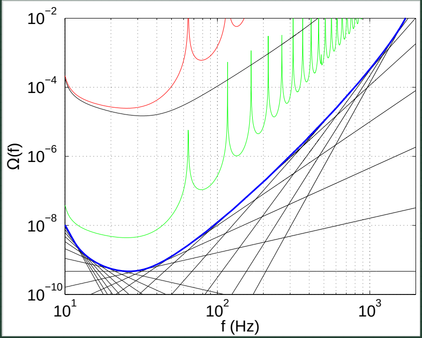

[Romano, Thrane: 1310.5300]

Black curve: Detector noise spectrum

$$D_{\rm noise}(f)$$

Red curve: Effective strain noise

$$S_{\rm noise}^{\rm eff}(f) = D_{\rm noise}(f) / \left|\Gamma(f)\right|$$

Green curve: Rescaled effective strain noise

$$S_{\rm noise}^{\rm eff}(f) / \sqrt{N_{\rm det}(N_{\rm det}-1)\, T\, \delta f}$$

Black straight lines: Set of power-law curves that result in $\varrho = 1$ based on Eq. (16)

Blue curve: Envelope $\rightarrow$ power-law-integrated sensitivity (PLIS) curve

$\rightarrow$ Power-law signals intersecting with the PLIS curve result in $\varrho > 1$.

---

[1] All curves expressed in terms of Ω: the GW energy density spectrum in units of the critical energy density ρ_c.

[2] Based on slightly obsolete data for $D_{\rm noise}$: `https://dcc.ligo.org/LIGO-T0900288/public`

Power-law-integrated sensitivity curves

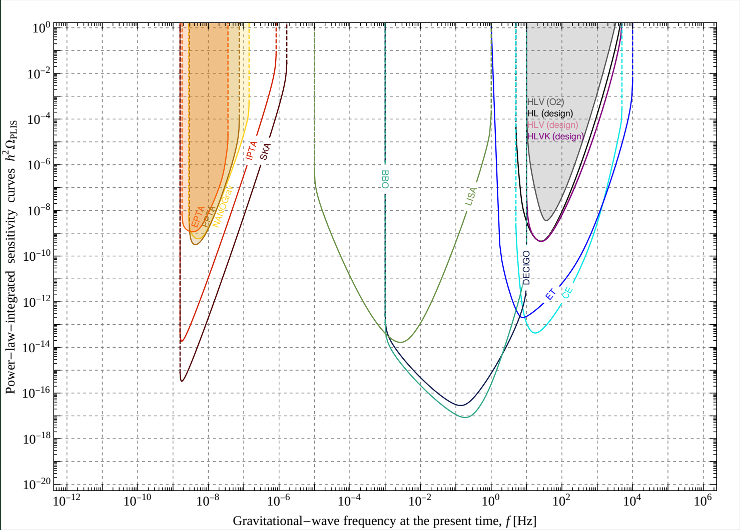

Sensitivity integrated over time and frequency, starting point of phenomenological studies

Pulsar timing

Use an array of pulsars across the Milky Way to construct a galaxy-sized GW detector![3]

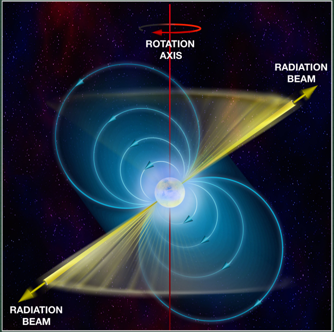

[B. Saxton for nrao.edu]

[3] First *indirect* detection of GWs from the orbital decay of the Hulse–Taylor binary (pulsar + neutron star).

Pulsar timing

Use an array of pulsars across the Milky Way to construct a galaxy-sized GW detector![3]

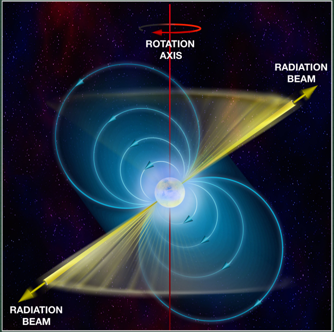

[B. Saxton for nrao.edu]

Pulsars: Highly magnetized rotating dead stars (usually neutron stars but also white dwarfs)

[3] First *indirect* detection of GWs from the orbital decay of the Hulse–Taylor binary (pulsar + neutron star).

Pulsar timing

Use an array of pulsars across the Milky Way to construct a galaxy-sized GW detector![3]

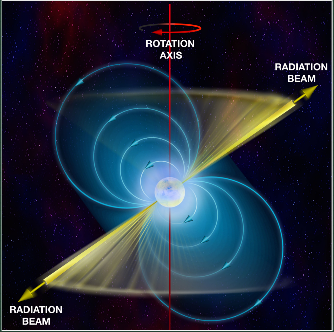

[B. Saxton for nrao.edu]

Pulsars: Highly magnetized rotating dead stars (usually neutron stars but also white dwarfs)

- Rotation periods of $10^{-3\cdots1}$ s. Accretion in close-binary systems → millisecond pulsars

[3] First *indirect* detection of GWs from the orbital decay of the Hulse–Taylor binary (pulsar + neutron star).

Pulsar timing

Use an array of pulsars across the Milky Way to construct a galaxy-sized GW detector![3]

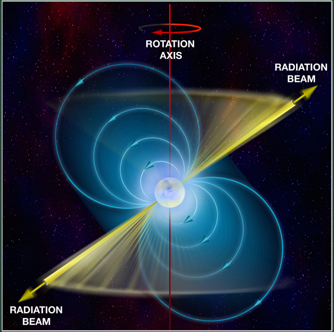

[B. Saxton for nrao.edu]

Pulsars: Highly magnetized rotating dead stars (usually neutron stars but also white dwarfs)

- Rotation periods of $10^{-3\cdots1}\,\mathrm{s}$. Accretion in close-binary systems $\rightarrow$ millisecond pulsars
- Beamed radio pulses emitted from magnetic poles $\rightarrow$ cosmic lighthouses

[3] First *indirect* detection of GWs from the orbital decay of the Hulse–Taylor binary (pulsar + neutron star).

Pulsar timing

Use an array of pulsars across the Milky Way to construct a galaxy-sized GW detector![3]

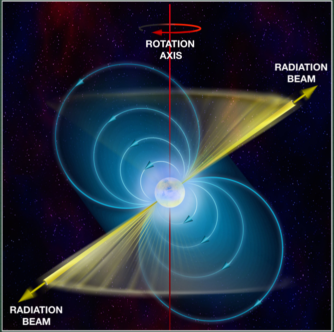

[B. Saxton for nrao.edu]

Pulsars: Highly magnetized rotating dead stars (usually neutron stars but also white dwarfs)

- Rotation periods of $10^{-3\cdots 1}\,\mathrm{s}$. Accretion in close-binary systems $\rightarrow$ millisecond pulsars
- Beamed radio pulses emitted from magnetic poles $\rightarrow$ cosmic lighthouses

Ultra-precise clocks in the sky! Look for tiny distortions caused by nanohertz GWs.

[3] First *indirect* detection of GWs from the orbital decay of the Hulse–Taylor binary (pulsar + neutron star).

Timing residuals

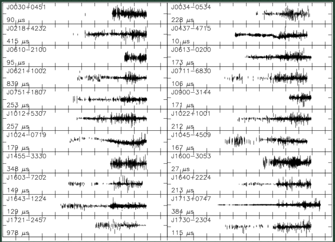

[IPTA Collaboration: 1602.03640]

Residuals in pulse times of arrival (TOAs):

$$R^{(i)} = \mathrm{TOA}^{(i)}_{\mathrm{SSB}} - \mathrm{TOA}^{(i)}_{\mathrm{Model}}$$

- Measure TOAs on earth and convert to TOAs at the solar-system barycenter (SSB)
- Compare to timing models for each pulsar (frequency and derivatives, position, proper motion, binary dynamics, relativistic effects, ...)

Timing residuals

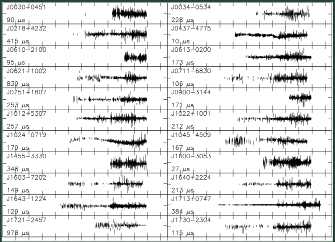

[IPTA Collaboration: 1602.03640]

Residuals in pulse times of arrival (TOAs):

$$R^{(i)} = \mathrm{TOA}^{(i)}_{\mathrm{SSB}} - \mathrm{TOA}^{(i)}_{\mathrm{Model}}$$

- Measure TOAs on earth and convert to TOAs at the solar-system barycenter (SSB)
- Compare to timing models for each pulsar (frequency and derivatives, position, proper motion, binary dynamics, relativistic effects, ...)

Timing noise of an idealized PTA experiment: $D_{\mathrm{noise}} = 2\,\sigma_t^2 \Delta T$

- $1/\Delta T$: Cadence of the observations; typically, ΔT of the order of a few weeks.
- σ_t: Root-mean-square error of the timing residuals; typically of the order of µs.

Timing residuals

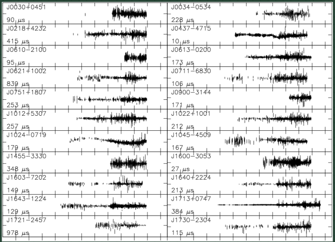

[IPTA Collaboration: 1602.03640]

Residuals in pulse times of arrival (TOAs):

$$R^{(i)} = \mathrm{TOA}^{(i)}_{\mathrm{SSB}} - \mathrm{TOA}^{(i)}_{\mathrm{Model}}$$

- Measure TOAs on earth and convert to TOAs at the solar-system barycenter (SSB)
- Compare to timing models for each pulsar (frequency and derivatives, position, proper motion, binary dynamics, relativistic effects, ...)

Timing noise of an idealized PTA experiment: $D_{\mathrm{noise}} = 2\,\sigma_t^2 \Delta T$

- $1/\Delta T$: Cadence of the observations; typically, ΔT of the order of a few weeks.
- σ_t: Root-mean-square error of the timing residuals; typically of the order of µs.

Sensitive to GWs in the frequency range: from $f_{\mathrm{min}} \sim 1/T$ to $f_{\mathrm{max}} \sim 1/\Delta T$

Timing residuals

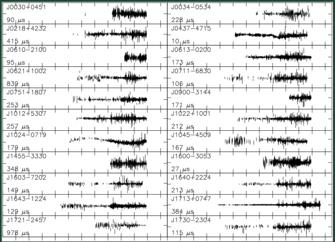

[IPTA Collaboration: 1602.03640]

Residuals in pulse times of arrival (TOAs):

$$R^{(i)} = \mathrm{TOA}^{(i)}_{\mathrm{SSB}} - \mathrm{TOA}^{(i)}_{\mathrm{Model}}$$

- Measure TOAs on earth and convert to TOAs at the solar-system barycenter (SSB)
- Compare to timing models for each pulsar (frequency and derivatives, position, proper motion, binary dynamics, relativistic effects, ...)

Timing noise of an idealized PTA experiment: $D_{\mathrm{noise}} = 2\,\sigma_t^2 \Delta T$

- $1/\Delta T$: Cadence of the observations; typically, ΔT of the order of a few weeks.
- σ_t: Root-mean-square error of the timing residuals; typically of the order of µs.

Sensitive to GWs in the frequency range: from $f_{\min} \sim 1/T$ to $f_{\max} \sim 1/\Delta T$

Existing PTA Collaborations:

EPTA + NANOGrav + PPTA = IPTA

Angular correlations

Integrate metric perturbation along the geodesic of the pulse $\rightarrow$ shift in pulsation frequency:

$$\frac{\Delta\nu(t)}{\nu} = -H^{ij}\left[h_{ij}(t,\boldsymbol{x}_e) - h_{ij}(t - D/c, \boldsymbol{x}_p)\right], \qquad R(t) = \int_0^t dt' \, \frac{\Delta\nu(t')}{\nu} \tag{17}$$

Two contributions: earth term, pulsar term (H^{ij}: geometrical factor; D: pulsar distance)

Angular correlations

Integrate metric perturbation along the geodesic of the pulse $\rightarrow$ shift in pulsation frequency:

$$\frac{\Delta\nu(t)}{\nu} = -H^{ij}\left[h_{ij}(t, \boldsymbol{x}_e) - h_{ij}(t - D/c, \boldsymbol{x}_p)\right], \qquad R(t) = \int_0^t dt' \, \frac{\Delta\nu(t')}{\nu} \tag{17}$$

Two contributions: earth term, pulsar term (H^{ij}: geometrical factor; D: pulsar distance)

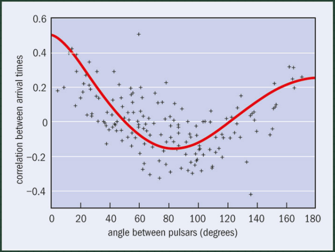

[Louise Mayor for physicsworld.com]

Cross-correlate the timing residuals of a pair of pulsars that is separated by an angle ψ in the sky:

$$\langle R_I \, R_J \rangle \propto \Gamma_{IJ}(\psi) = \frac{\zeta_{IJ}(\psi)}{12\pi^2 f^2} \tag{18}$$

Angular correlations

Integrate metric perturbation along the geodesic of the pulse $\rightarrow$ shift in pulsation frequency:

$$\frac{\Delta\nu(t)}{\nu} = -H^{ij}\left[h_{ij}(t, \boldsymbol{x}_e) - h_{ij}(t - D/c, \boldsymbol{x}_p)\right], \qquad R(t) = \int_0^t dt' \, \frac{\Delta\nu(t')}{\nu} \tag{17}$$

Two contributions: earth term, pulsar term (H^{ij}: geometrical factor; D: pulsar distance)

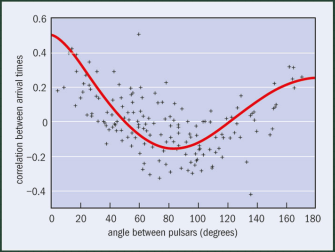

[Louise Mayor for physicsworld.com]

Cross-correlate the timing residuals of a pair of pulsars that is separated by an angle ψ in the sky:

$$\langle R_I \, R_J \rangle \propto \Gamma_{IJ}(\psi) = \frac{\zeta_{IJ}(\psi)}{12\pi^2 f^2} \tag{18}$$

Earth term results in characteristic correlation:

$$\zeta_{IJ}(\psi) = \frac{1}{2}\left[\delta_{IJ} + 1 + c_\psi \left(3 \, \ln c_\psi - \frac{1}{2}\right)\right] \tag{19}$$

with $c_\psi = (1 - \cos\psi)/2$. Hellings–Downs curve!

[Hellings, Downs: Astrophys. J. 265 (1983) L39]]

Angular correlations

Integrate metric perturbation along the geodesic of the pulse $\rightarrow$ shift in pulsation frequency:

$$\frac{\Delta\nu(t)}{\nu} = -H^{ij}\left[h_{ij}(t, \boldsymbol{x}_e) - h_{ij}(t - D/c, \boldsymbol{x}_p)\right] , \qquad R(t) = \int_0^t dt' \, \frac{\Delta\nu(t')}{\nu} \tag{17}$$

Two contributions: earth term, pulsar term (H^{ij}: geometrical factor; D: pulsar distance)

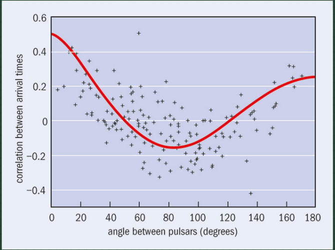

[Louise Mayor for physicsworld.com]

Cross-correlate the timing residuals of a pair of pulsars that is separated by an angle ψ in the sky:

$$\langle R_I \, R_J \rangle \propto \Gamma_{IJ}(\psi) = \frac{\zeta_{IJ}(\psi)}{12\pi^2 f^2} \tag{18}$$

Earth term results in characteristic correlation:

$$\zeta_{IJ}(\psi) = \frac{1}{2}\left[\delta_{IJ} + 1 + c_\psi \left(3 \, \ln c_\psi - \frac{1}{2}\right)\right] \tag{19}$$

with $c_\psi = (1 - \cos\psi)/2$. Hellings–Downs curve!

[Hellings, Downs: Astrophys. J. 265 (1983) L39]]

Hallmark signature of a SGWB signal: Quadrupole correlation among timing residuals.

Other systematic effects typically lead to monopole or dipole correlations (see Lecture 3B).

Imprint of primordial GWs on the CMB

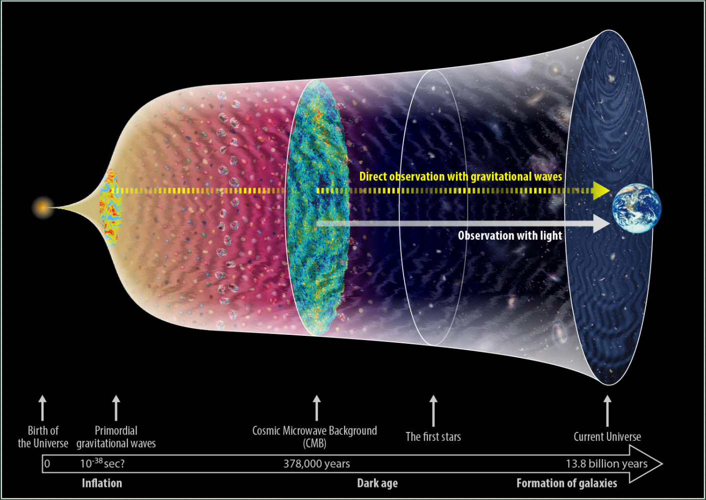

[National Astronomical Observatory of Japan, gwpo.nao.ac.jp]

Probe GWs with oscillation periods of billions of years! (Inflation, topological defects, ...)

Imprint of primordial GWs on the CMB

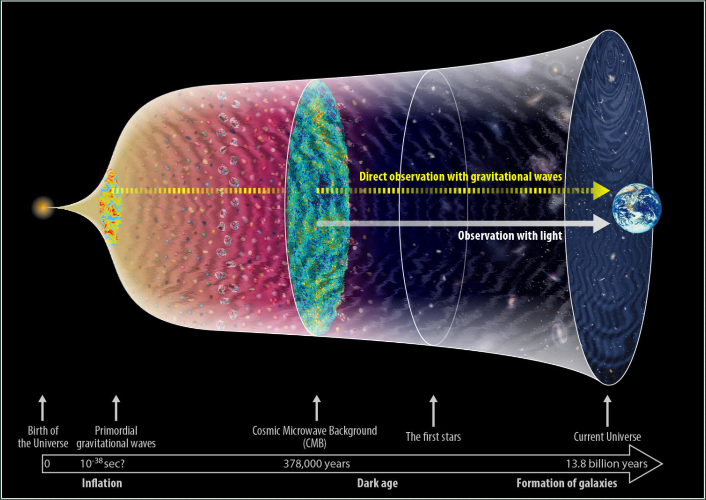

[National Astronomical Observatory of Japan, gwpo.nao.ac.jp]

Probe GWs with oscillation periods of billions of years! (Inflation, topological defects, ...)

- Temperature anisotropies ▪ Polarization anisotropies ▪ Spectral distortions

Temperature anisotropies

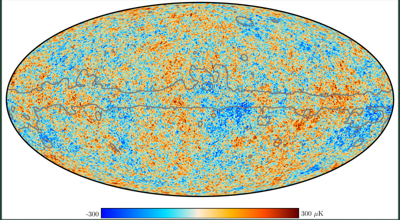

[PLANCK Collaboration, cosmos.esa.int]

CMB: Baby picture of the early Universe, surface of last scattering after recombination

Temperature anisotropies

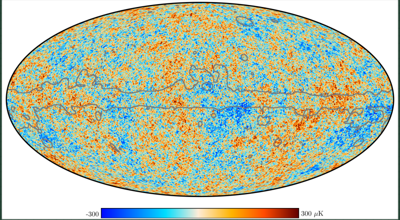

[PLANCK Collaboration, cosmos.esa.int]

CMB: Baby picture of the early Universe, surface of last scattering after recombination

Highly isotropic, temperature anisotropies:

$$\Theta = \frac{\Delta T}{\bar{T}} \sim 10^{-5}\,, \qquad \bar{T} \simeq 2.725\,\mathrm{K} \tag{20}$$

Temperature anisotropies

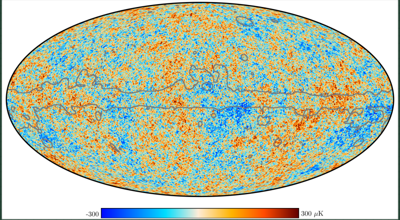

[PLANCK Collaboration, cosmos.esa.int]

CMB: Baby picture of the early Universe, surface of last scattering after recombination

Highly isotropic, temperature anisotropies:

$$\Theta = \frac{\Delta T}{\bar{T}} \sim 10^{-5}\,, \qquad \bar{T} \simeq 2.725\,\mathrm{K} \tag{20}$$

Expand in spherical harmonics:

$$\Theta(\boldsymbol{n}) = \sum_{\ell=0}^{\infty} \sum_{m=-\ell}^{+\ell} \Theta_{\ell m} Y_{\ell m}(\boldsymbol{n}) \tag{21}$$

Temperature anisotropies

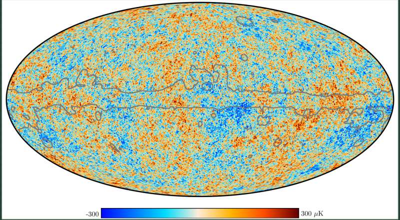

[PLANCK Collaboration, cosmos.esa.int]

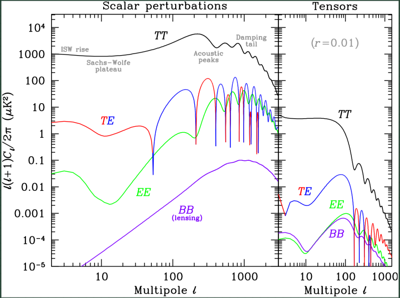

[Review of Particle Physics (2020), pdg.lbl.gov]

CMB: Baby picture of the early Universe, surface of last scattering after recombination

Highly isotropic, temperature anisotropies:

$$\Theta = \frac{\Delta T}{\bar{T}} \sim 10^{-5}\,, \qquad \bar{T} \simeq 2.725\,\mathrm{K} \qquad (20)$$

Expand in spherical harmonics:

$$\Theta(\boldsymbol{n}) = \sum_{\ell=0}^{\infty} \sum_{m=-\ell}^{+\ell} \Theta_{\ell m} Y_{\ell m}(\boldsymbol{n}) \qquad (21)$$

Power spectrum describing average $\Theta_{\ell m}$:

$$\langle \Theta_{\ell m} \Theta^*_{\ell' m'} \rangle = \delta_{\ell\ell'}\, \delta_{mm'}\, C_\ell^{TT} \qquad (22)$$

Temperature anisotropies

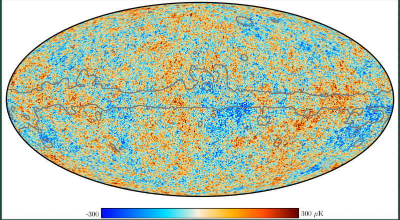

[PLANCK Collaboration, cosmos.esa.int]

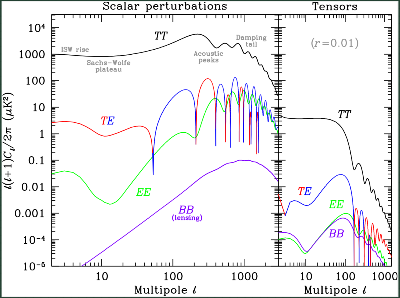

[Review of Particle Physics (2020), pdg.lbl.gov]

CMB: Baby picture of the early Universe, surface of last scattering after recombination

Highly isotropic, temperature anisotropies:

$$\Theta = \frac{\Delta T}{\bar{T}} \sim 10^{-5}\,, \qquad \bar{T} \simeq 2.725\,\mathrm{K} \qquad (20)$$

Expand in spherical harmonics:

$$\Theta(\boldsymbol{n}) = \sum_{\ell=0}^{\infty} \sum_{m=-\ell}^{+\ell} \Theta_{\ell m} Y_{\ell m}(\boldsymbol{n}) \qquad (21)$$

Power spectrum describing average $\Theta_{\ell m}$:

$$\langle \Theta_{\ell m} \Theta^{*}_{\ell' m'} \rangle = \delta_{\ell\ell'}\, \delta_{mm'}\, C_\ell^{TT} \qquad (22)$$

Tensor perturbations induce C_ℓ^{TT} through the Sachs–Wolfe effect (gravitational redshift):

$$\Theta = -\int_{\mathrm{CMB}}^{\mathrm{today}} d\lambda\, h'_{ij}(\eta, \boldsymbol{x})\, n^i n^j \qquad (23)$$

Polarization anisotropies

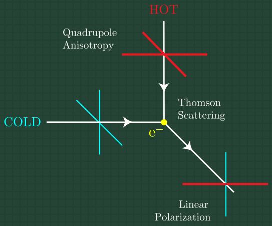

[Hu, White: astro-ph/9706147]

Tensor perturbations → quadrupole temperature anisotropy
→ Thomson scattering results in linear CMB polarization

Polarization anisotropies

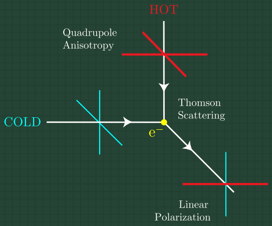

[Hu, White: astro-ph/9706147]

Tensor perturbations $\rightarrow$ quadrupole temperature anisotropy $\rightarrow$ Thomson scattering results in linear CMB polarization

Decompose polarization field into E mode and B mode:

$$\boldsymbol{\nabla} \times \boldsymbol{E} = 0\,, \qquad \boldsymbol{\nabla} \cdot \boldsymbol{B} = 0 \tag{24}$$

Polarization anisotropies

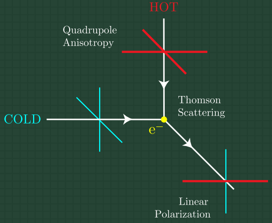

[Hu, White: astro-ph/9706147]

Tensor perturbations → quadrupole temperature anisotropy → Thomson scattering results in linear CMB polarization

Decompose polarization field into E mode and B mode:

$$\boldsymbol{\nabla} \times \boldsymbol{E} = 0\,, \qquad \boldsymbol{\nabla} \cdot \boldsymbol{B} = 0 \tag{24}$$

Possible sources:
E mode: Scalar and tensor perturbations
B mode: Lensed E modes (✓) and tensor perturbations (?)

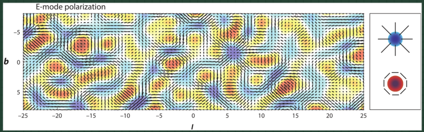

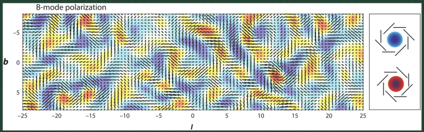

[Kamionkowski, Kovetz: Annual Review of Astronomy and Astrophysics **54** (2016) 227]

Polarization anisotropies

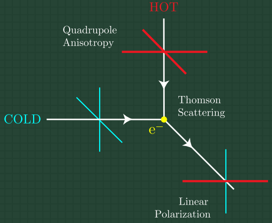

[Hu, White: astro-ph/9706147]

Tensor perturbations → quadrupole temperature anisotropy
→ Thomson scattering results in linear CMB polarization

Decompose polarization field into E mode and B mode:

$$\nabla \times \boldsymbol{E} = 0\,, \qquad \nabla \cdot \boldsymbol{B} = 0 \tag{24}$$

Possible sources:
E mode: Scalar and tensor perturbations
B mode: Lensed E modes (✓) and tensor perturbations (?)

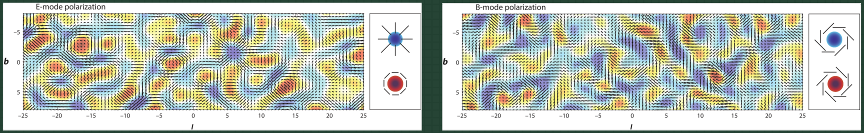

[Kamionkowski, Kovetz: Annual Review of Astronomy and Astrophysics **54** (2016) 227]

Strength of tensor perturbations on CMB scales in terms of tensor-to-scalar ratio r:

$$r = \frac{\mathcal{P}_h(k_*)}{\mathcal{P}_\mathcal{R}(k_*)}\,, \qquad \langle \mathcal{R}\mathcal{R}^* \rangle = \frac{2\pi^2}{k^3}\,\delta^{(3)}\,\mathcal{P}_\mathcal{R}(k)\,, \qquad \langle h_{ij} h_{ij}^* \rangle = \frac{2\pi^2}{k^3}\,\delta^{(3)}\,\mathcal{P}_h(k) \tag{25}$$

Best limit to date (PLANCK and BICEP/Keck): $r(k_* = 0.05\,\mathrm{Mpc}^{-1}) < 0.044$ at $95\,\%$ C. L.

[Tristram et al.: 2010.01139]

Spectral distortions

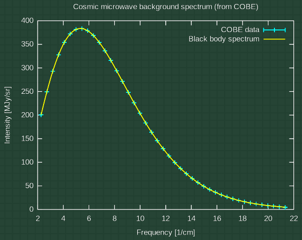

[commons.wikimedia.org]

CMB: Best blackbody spectrum in nature

Spectral distortions

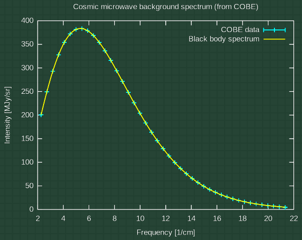

[commons.wikimedia.org]

CMB: Best blackbody spectrum in nature

Tensor perturbations dissipate; energy transfer to photons at $z \lesssim 2 \times 10^6$ when n_γ constant leads to μ-distortion: Bose–Einstein distribution with $\mu \neq 0$:

$$f(E) = \frac{1}{e^{(E-\mu)/T} - 1} \qquad (26)$$

$$\langle \mu \rangle = \int \frac{dk}{k} W(k)\, \mathcal{P}_h(k) \qquad (27)$$

Spectral distortions

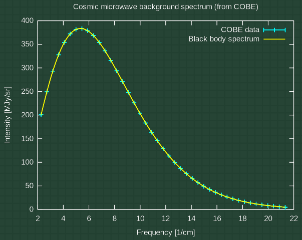

[commons.wikimedia.org]

CMB: Best blackbody spectrum in nature

Tensor perturbations dissipate; energy transfer to photons at $z \lesssim 2 \times 10^6$ when n_γ constant leads to μ-distortion: Bose–Einstein distribution with $\mu \neq 0$:

$$f(E) = \frac{1}{e^{(E-\mu)/T} - 1} \tag{26}$$

$$\langle \mu \rangle = \int \frac{dk}{k}\, W(k)\, \mathcal{P}_h(k) \tag{27}$$

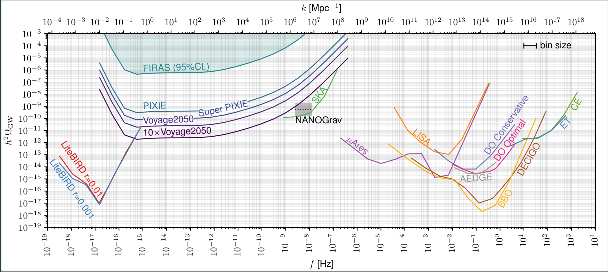

[Kite, Ravenni, Patil, Chluba: 2010.00040]

Future CMB spectrometers:

Bridge the gap between cosmological and astrophysical GW searches!

$$f \sim 10^{-15} \cdots 10^{-9}\ \mathrm{Hz}$$

Summary Lecture 1B

Take-home messages:

Summary Lecture 1B

Take-home messages:

- The global network of GW detectors is growing; soon multifrequency GW astronomy.

Summary Lecture 1B

Take-home messages:

- The global network of GW detectors is growing; soon multifrequency GW astronomy.
- Signal response quantified in terms of detector transfer / overlap reduction functions.

Summary Lecture 1B

Take-home messages:

- The global network of GW detectors is growing; soon multifrequency GW astronomy.
- Signal response quantified in terms of detector transfer / overlap reduction functions.
- Cross-correlation analysis to search for a stochastic GW signal with a detector network.

Summary Lecture 1B

Take-home messages:

- The global network of GW detectors is growing; soon multifrequency GW astronomy.
- Signal response quantified in terms of detector transfer / overlap reduction functions.
- Cross-correlation analysis to search for a stochastic GW signal with a detector network.
- Optimal SNR requires matched filter based on the actual signal $\rightarrow$ template banks.

Summary Lecture 1B

Take-home messages:

- The global network of GW detectors is growing; soon multifrequency GW astronomy.
- Signal response quantified in terms of detector transfer / overlap reduction functions.
- Cross-correlation analysis to search for a stochastic GW signal with a detector network.
- Optimal SNR requires matched filter based on the actual signal $\rightarrow$ template banks.
- Different types of sensitivity curves: (effective) strain noise, power-law-integrated, ...

Summary Lecture 1B

Take-home messages:

- The global network of GW detectors is growing; soon multifrequency GW astronomy.
- Signal response quantified in terms of detector transfer / overlap reduction functions.
- Cross-correlation analysis to search for a stochastic GW signal with a detector network.
- Optimal SNR requires matched filter based on the actual signal $\rightarrow$ template banks.
- Different types of sensitivity curves: (effective) strain noise, power-law-integrated, ...
- PTAs seek to measure Hellings–Downs correlation among pulsar timing residuals.

Summary Lecture 1B

Take-home messages:

- The global network of GW detectors is growing; soon multifrequency GW astronomy.
- Signal response quantified in terms of detector transfer / overlap reduction functions.
- Cross-correlation analysis to search for a stochastic GW signal with a detector network.
- Optimal SNR requires matched filter based on the actual signal $\rightarrow$ template banks.
- Different types of sensitivity curves: (effective) strain noise, power-law-integrated, ...
- PTAs seek to measure Hellings–Downs correlation among pulsar timing residuals.
- CMB: temperature / polarization anisotropies (B modes!), spectral μ-distortions.

Summary Lecture 1B

Take-home messages:

- The global network of GW detectors is growing; soon multifrequency GW astronomy.
- Signal response quantified in terms of detector transfer / overlap reduction functions.
- Cross-correlation analysis to search for a stochastic GW signal with a detector network.
- Optimal SNR requires matched filter based on the actual signal $\rightarrow$ template banks.
- Different types of sensitivity curves: (effective) strain noise, power-law-integrated, ...
- PTAs seek to measure Hellings–Downs correlation among pulsar timing residuals.
- CMB: temperature / polarization anisotropies (B modes!), spectral μ-distortions.
- Meaning of $h^2\Omega_{\rm GW}$ ($\checkmark$), experimental sensitivity curves in plots of $h^2\Omega_{\rm GW}(f)$ ($\checkmark$).

Summary Lecture 1B

Take-home messages:

- The global network of GW detectors is growing; soon multifrequency GW astronomy.
- Signal response quantified in terms of detector transfer / overlap reduction functions.
- Cross-correlation analysis to search for a stochastic GW signal with a detector network.
- Optimal SNR requires matched filter based on the actual signal $\rightarrow$ template banks.
- Different types of sensitivity curves: (effective) strain noise, power-law-integrated, ...
- PTAs seek to measure Hellings–Downs correlation among pulsar timing residuals.
- CMB: temperature / polarization anisotropies (B modes!), spectral μ-distortions.
- Meaning of $h^2\Omega_{\mathrm{GW}}$ (✓), experimental sensitivity curves in plots of $h^2\Omega_{\mathrm{GW}}(f)$ (✓).

End of Lecture 1B. Thanks a lot for your attention!